

# ToF–SIMS depth profiling analysis of the uptake of Ba<sup>2+</sup> and Co<sup>2+</sup> ions by natural kaolinite clay

T. Shahwan<sup>a,\*</sup>, H.N. Erten<sup>b</sup>, L. Black<sup>c</sup>, G.C. Allen<sup>c</sup>

<sup>a</sup> Department of Chemistry, Izmir Institute of Technology, 35430 Urla, Izmir, Turkey

<sup>b</sup> Department of Chemistry, Bilkent University, 06533 Bilkent, Ankara, Turkey

<sup>c</sup> Interface Analysis Centre, University of Bristol, 121 St. Michael's Hill, Bristol, UK

Received 14 January 2004; accepted 12 April 2004

Available online 7 May 2004

## Abstract

The sorption behavior of Ba<sup>2+</sup> and Co<sup>2+</sup> ions on a natural clay sample rich in kaolinite was studied using time-of-flight secondary ion mass spectrometry (ToF–SIMS). Depth profiling at 10-Å steps was performed up to a 70-Å matrix depth of the clay prior to and following sorption. The results showed that Co<sup>2+</sup> is sorbed in slightly larger quantities than Ba<sup>2+</sup>, with significant numbers of ions fixed on the outermost surface of the clay. Depletion of the ions K<sup>+</sup>, Mg<sup>2+</sup>, and Ca<sup>2+</sup> from the clay lattice was observed to accompany enrichment with Co<sup>2+</sup> and Ba<sup>2+</sup> ions. The data obtained using X-ray powder diffraction (XRPD) and scanning electron microscopy (SEM) indicated insignificant structural and morphological changes in the lattice of the clay upon sorption of both Ba<sup>2+</sup> and Co<sup>2+</sup> ions. Analysis using energy dispersive X-ray spectroscopy (EDS) showed that the average atomic percentage ( $\pm$ S.D.) of Ba and Co on kaolinite surface were  $0.49 \pm 0.11$  and  $0.61 \pm 0.19$ , respectively, indicating a limited uptake capacity of natural kaolinite for both ions.

© 2004 Elsevier Inc. All rights reserved.

**Keywords:** Ba; Co; Sorption; Kaolinite; Depth Profiling; ToF–SIMS

## 1. Introduction

The elements Ba and Co have the important corresponding radioisotopes <sup>140</sup>Ba and <sup>60</sup>Co. <sup>140</sup>Ba ( $t_{1/2} = 14.8$  days) is produced in high yield during nuclear fission reactions. <sup>60</sup>Co ( $t_{1/2} = 5.3$  yr) is formed by activation of <sup>59</sup>Co in nuclear materials and is widely used in medical treatment. Both isotopes are important from the viewpoint of radioactive waste disposal, as their migration from the disposal site and their mixing with underground water could create a serious impact on the surrounding biological environment. Kaolinite, among other clays found around various kinds of geological repositories, is one of the natural buffering materials that might retard or delay the migration of such harmful radionuclides into the biosphere.

The ideal formula of kaolinite is Al<sub>2</sub>Si<sub>2</sub>O<sub>5</sub>(OH)<sub>4</sub>, and most minerals of the kaolin group appear to be close to ideal in composition. The structure of kaolinite consists of stacked

units, each composed of one octahedrally coordinated sheet of aluminum ions and one tetrahedrally coordinated sheet of silicon ions (a 1:1 clay mineral). When these layers stack, the OH<sup>-</sup> ions on one structural unit lie next to and in close contact with the O<sup>2-</sup> plane of its neighbor structural unit. As a result, the structure becomes tightly bound via hydrogen bonding, the thing that makes kaolinite a nonexpanding clay, thus limiting sorption on the interlayer positions of this clay and yielding a low CEC. The unit layer of kaolinite is about 7 Å thick, which gives rise to a characteristic X-ray diffraction peak corresponding to about 7 Å [1].

In this study, the sorption behavior of Ba<sup>2+</sup> and Co<sup>2+</sup> on a natural sample of kaolinite is studied using time-of-flight secondary ion mass spectrometry (ToF–SIMS). The technique was helpful in mapping the surface of the clay. Quantification of the depletion of different elements initially contained within the analyzed clay surface enabled evaluation of the role of ion exchange in the sorption process. X-ray powder diffraction (XRPD) was applied to examine the mineralogical composition of natural kaolinite and to detect any possible structural changes that might take place in the clay

\* Corresponding author. Fax: +90-232-7507509.

E-mail address: [talalshahwan@iyte.edu.tr](mailto:talalshahwan@iyte.edu.tr) (T. Shahwan).

following sorption. Scanning electron microscopy (SEM) was used to reveal the possible morphological changes of the clay before and after sorption.

ToF–SIMS was applied earlier to study the sorption behavior of these ions on natural clay samples rich in chlorite–illite and bentonite clays [2,3] and of  $\text{Cs}^+$  on natural kaolinite [4]. In dealing with geological samples, the most important difficulty associated with the application of surface-sensitive techniques stems from the heterogeneous nature of such samples. To overcome this problem, the measurements were performed at randomly selected locations and the values outlined in this study correspond to arithmetic averages of the measured magnitudes.

## 2. Experimental

The natural clay mineral samples were obtained from the Turkish General Directorate of Mineral Research and Exploration (MTA). The clay minerals originated from the Sındirgi region of Turkey, located in the western part of Anatolia. The particle size of the clay samples used in the experiments was  $<38\ \mu\text{m}$ . The batch method was used throughout the study.

Prior to the sorption experiments, the clay was characterized using XRPD and SEM techniques. In the XRPD experiments, the clay samples were first ground and mounted on metallic disk holders, with methanol used to disperse the powder grains evenly over the holder. The samples were then introduced for analysis into a Rigaku miniflex X-ray diffractometer. In the instrument, the source consisted of  $\text{CuK}\alpha$  radiation, generated in a tube operating at 30 kV and 15 mA. The figures were recorded with  $2\theta$  values ranging from  $2^\circ$  to  $50^\circ$  in steps of  $0.02^\circ$  with dwell times of 10 s per step. The effect of grain orientation on the recorded diagrams was checked by preparing different samples and analyzing them under the same conditions. The results showed no significant difference in the peak intensities or peak positions.

The SEM/EDS characterization was performed using a Philips XL-30S FEG type instrument located at the Center of Material Research at Izmir Institute of Technology. The clay samples were first sprinkled onto adhesive carbon tapes supported on metallic disks and then coated using deposited Au–Pd vapor. Microimages of the sample surfaces were then recorded at different magnifications.

The sorption experiments were carried out by mixing 400.0-ml aliquots of 0.010 M  $\text{BaCl}_2$  or 0.010 M  $\text{Co}(\text{NO}_3)_2$  with powdered kaolinite samples weighing 4.0 g each for 48 h using a magnetic stirrer. The samples were then filtered using Whatman filter papers (No. 5) and dried overnight at  $90^\circ\text{C}$ . The pH at the start of the sorption experiments was in the range  $\sim 6.5$ – $8$  higher than the isoelectric point (IEP) of kaolinite ( $\sim 3.5$ ).

ToF–SIMS analysis of the natural and Ba- and Co-loaded clay samples was performed using a vacuum generator ToF–SIMS instrument located at the Interface Surface Analysis Centre at the University of Bristol. During analysis, the vac-

uum in the analysis chamber was kept at approximately  $10^{-9}$  mbar. Spectra were recorded over 50 accumulations, at  $\times 5000$  magnification, i.e., an area of  $64 \times 48$  mm. The ion-beam pulse length was 30 ns with a repetition rate of 10 kHz. The  $\text{Ga}^+$  ion gun used to produce the ions was operated at 1 nA current and 20 keV energy. The electron flood gun was used as required for neutralization. These conditions resulted in an etching rate of approximately  $10\ \text{\AA}$  per 50-s etch. The samples were etched and analysis was performed at successive depths of 10, 20, 30, 40, 50, and  $70\ \text{\AA}$ . MS Origin 50 was used in carrying out the quantification analysis of the ToF–SIMS data

Quantitative analysis using ToF–SIMS is usually affected by various instrumental and matrix complications that might affect the measurements. Usually, the relative sensitivity corrections performed for individual elements are believed to fold most of the errors created by instrumental effects as long as the samples are analyzed under identical operating conditions. One of the difficulties caused by the nature of the analyzed clay matrix resulted from the implantation of  $\text{Ga}_2^+$  ions on the analyzed sample by the  $\text{Ga}^+$  primary ion beam. This has caused interference of  $\text{Ga}_2^+$  ( $A = 138$ ) with the major isotope of Ba (71.7%) having the same mass number. Calculating the ratios of peak intensities of  $^{138}\text{Ba}$  to those of other Ba isotopes and comparing them with the natural isotopic ratios confirmed this interference. Consequently other Ba isotopes were used in the calculations ( $^{137}\text{Ba}$  and  $^{134}\text{Ba}$ ) and correction to 100% abundance was performed. Another difficulty was caused by the fact that poorly conducting materials, as in our case, usually suffer from the problem of charging, i.e., the buildup of positive charge on the analyzed surface as a result of bombardment by the primary ion beam. Charge buildup during analysis can cause secondary ions with narrow energy distributions (e.g., alkali metals, alkaline earths) to shift outside the optimum transmittance window of the spectrometer, thus lowering their yield [5]. The effect of charging was accounted for by applying an electron gun to flood the surface with low-energy electrons, compensating for the deposited positive charge. To avoid any inconsistency in the experimental data that can be caused by surface heterogeneity and/or grain orientation of the clay particles, etching was performed at different locations of the analyzed sample. Average results were then corrected using the corresponding relative sensitivity factors (RSF) [6]. Table 1 gives the isotopes of the analyzed elements together with the relative sensitivity factors of these elements. The corrected data were then expressed relative to (Al + Si) content, assuming that both Al and Si skeletal elements are nonexchanging.

## 3. Results and discussion

The XRPD diagrams of the natural clay sample showed that it was composed mainly of kaolinite, in addition to quartz. Kaolinite is characterized by the 001 and 002 main features appearing at  $d_{001} = 7.15\ \text{\AA}$  and  $d_{002} = 3.57\ \text{\AA}$ . The

Table 1  
The elements considered in ToF-SIMS calculations: relative sensitivity factors and natural stable isotopes

| Element | RSF  | Natural isotope(s)  | % Abundance                        |
|---------|------|---|------------------------------------|
| Mg      | 160  | <sup>24</sup> Mg, <sup>25</sup> Mg, <sup>26</sup> Mg  | 78.6, 10.1, 11.3                   |
| Al      | 120  | <sup>27</sup> Al  | 100                                |
| Si      | 27   | <sup>28</sup> Si, <sup>29</sup> Si, <sup>30</sup> Si  | 92.2, 4.7, 3.1                     |
| K       | 1800 | <sup>39</sup> K, <sup>41</sup> K  | 93.1, 6.9                          |
| Ca      | 250  | <sup>40</sup> Ca, <sup>42</sup> Ca, <sup>43</sup> Ca, <sup>44</sup> Ca,<br><sup>46</sup> Ca, <sup>48</sup> Ca       | 97.0, 0.6, 0.1, 2.1,<br>0.003, 0.2 |
| Fe      | 21   | <sup>54</sup> Fe, <sup>56</sup> Fe, <sup>57</sup> Fe, <sup>58</sup> Fe  | 5.8, 91.7, 2.2, 0.3                |
| Ba      | 90   | <sup>132</sup> Ba, <sup>134</sup> Ba, <sup>135</sup> Ba,<br><sup>136</sup> Ba, <sup>137</sup> Ba, <sup>138</sup> Ba | 0.1, 2.4, 6.6, 7.8,<br>11.3, 71.7  |
| Co      | 23   | <sup>59</sup> Co  | 100                                |

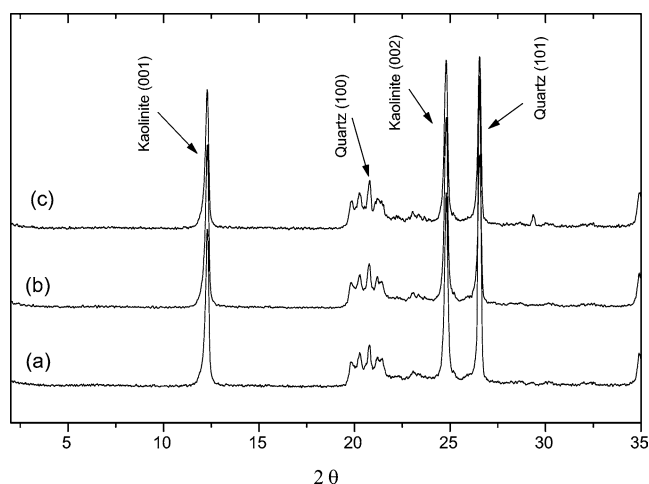


Fig. 1. XRD diagrams of (a) natural kaolinite, (b) Ba-sorbed kaolinite, and (c) Co-sorbed kaolinite.

diagram of the natural clay is given in Fig. 1a. The sharp features indicate good crystallinity, the property supported by the SEM microimage shown in Fig. 2. The peak arising at  $d_{101} = 3.34 \text{ \AA}$  in the XRPD diagram corresponds to the major feature of the quartz impurity in the natural clay sample.

The chemical content of the clay was obtained using the semiquantitative EDS data, which showed that the natural clay is composed of MgO, Al<sub>2</sub>O<sub>3</sub>, SiO<sub>2</sub>, K<sub>2</sub>O, CaO, and Fe<sub>2</sub>O<sub>3</sub>. The average amounts of these components (mol% ± S.D.) were  $2.7 \pm 0.3$ ,  $29.7 \pm 1.4$ ,  $65.5 \pm 3.9$ ,  $0.5 \pm 0.2$ ,  $1.4 \pm 0.3$ ,  $0.2 \pm 0.2$ , respectively. Elements such as Mg, K, Ca, and Fe are usually not encountered in the structure of pure kaolinite. Their presence in the natural clay might be indicative of the presence of minor quantities of other minerals (possibly smectite-like) that are below the detection limit (~5%) of the XRPD technique.

A typical ToF-SIMS spectrum of the natural clay sample of kaolinite is given in Fig. 3. The two insets in the figure show the variation of Ba and Co signals at various depths. The analysis showed that the enrichment of the clay surface with Ba<sup>2+</sup> and Co<sup>2+</sup> ions was associated with a decrease in the contents of K<sup>+</sup>, Mg<sup>2+</sup>, and Ca<sup>2+</sup> originally present in the

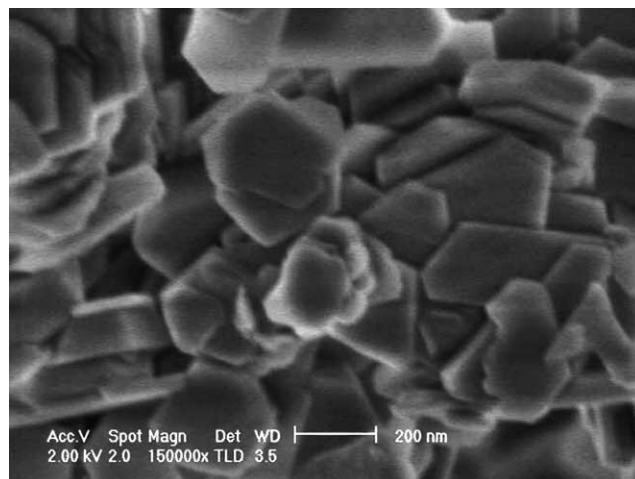


Fig. 2. SEM micrograph obtained at  $\times 150,000$  magnification for the natural kaolinite used in this study.

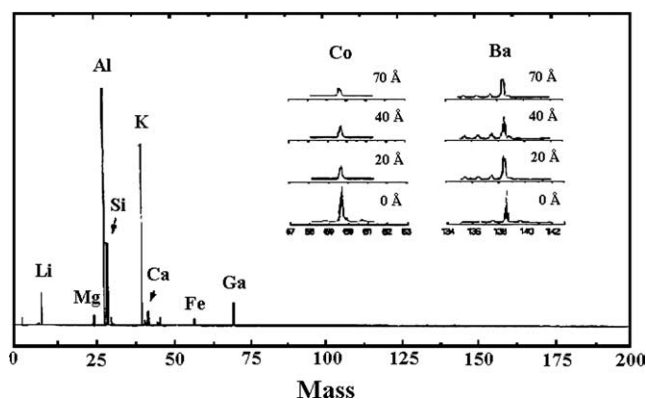


Fig. 3. A typical ToF-SIMS spectrum of the clay sample before sorption. The insets show the variation of sorbed Ba<sup>2+</sup> and Co<sup>2+</sup> signals on the clay at different depths.

natural clay. The amounts of these ions before and after the sorption experiments are given in Table 2. The term EDA in the table corresponds to the equivalent depleted amount of cation  $x$ . Each EDA value is calculated by multiplying the difference  $[(R_i)_x - (R_f)_x]$  by  $z_x$ , the charge of cation  $x$ . The EDA values for K<sup>+</sup>, Mg<sup>2+</sup>, and Ca<sup>2+</sup> show that while Ca<sup>2+</sup> depletion is higher near the uppermost surface, that of K<sup>+</sup> becomes more significant in the deeper sites. The behavior of Mg<sup>2+</sup> tends—to a certain extent—to resemble that of Ca<sup>2+</sup>.

The amounts of Ba<sup>2+</sup> and Co<sup>2+</sup> ions sorbed on natural kaolinite as a function of matrix depth are shown in Fig. 4. The error bars in the figure were used to account for the maximum deviation of the data from the mean values, which were calculated after analysis at different points on the loaded kaolinite surface. The figure indicates higher sorption of the two cations on the uppermost clay surface. The cation sorbed by the uppermost surface as a percentage of its total sorbed amount is 20% and 28% for Ba<sup>2+</sup> and Co<sup>2+</sup> sorption, respectively. These quantities were calculated by dividing the sorbed amount of each cation at the outer surface (0 Å) by the total sorbed amounts within the

Table 2

The initial and final ratios of cation/(Al + Si),  $R_i$ ,  $R_f$ , and the equivalent depleted amounts (EDA) as a function of depth for the sorption of  $Ba^{2+}$ , and  $Co^{2+}$  on kaolinite

| Cation            | Depth (Å) | $R_i$  | Ba sorption |        | Co sorption |        |
|-------------------|-----------|--------|-------------|--------|-------------|--------|
|                   |           |        | $R_f$       | EDA    | $R_f$       | EDA    |
| $K^+$             | 0         | 0.0131 | 0.0068      | 0.0063 | 0.0061      | 0.0070 |
|                   | 10        | 0.0275 | 0.0151      | 0.0124 | 0.0202      | 0.0073 |
|                   | 20        | 0.0314 | 0.0148      | 0.0166 | 0.0195      | 0.0119 |
|                   | 30        | 0.0314 | 0.0145      | 0.0169 | 0.0199      | 0.0115 |
|                   | 40        | 0.0313 | 0.0144      | 0.0169 | 0.0168      | 0.0145 |
|                   | 50        | 0.0292 | 0.0149      | 0.0143 | 0.0165      | 0.0127 |
|                   | 70        | 0.0277 | 0.0141      | 0.0136 | 0.0141      | 0.0136 |
| Total             |           |        |             | 0.0970 |             | 0.0785 |
| $Mg^{2+}$         | 0         | 0.0239 | 0.0127      | 0.0224 | 0.0079      | 0.0320 |
|                   | 10        | 0.0143 | 0.0088      | 0.0110 | 0.0060      | 0.0166 |
|                   | 20        | 0.0124 | 0.0079      | 0.0090 | 0.0059      | 0.0130 |
|                   | 30        | 0.0126 | 0.0078      | 0.0096 | 0.0055      | 0.0142 |
|                   | 40        | 0.0120 | 0.0081      | 0.0078 | 0.0057      | 0.0126 |
|                   | 50        | 0.0128 | 0.0083      | 0.0090 | 0.0060      | 0.0136 |
|                   | 70        | 0.0125 | 0.0081      | 0.0088 | 0.0055      | 0.0140 |
| Total             |           |        |             | 0.0776 |             | 0.1160 |
| $Ca^{2+}$         | 0         | 0.0241 | 0.0050      | 0.0382 | 0.0056      | 0.0370 |
|                   | 10        | 0.0077 | 0.0021      | 0.0112 | 0.0025      | 0.0104 |
|                   | 20        | 0.0070 | 0.0018      | 0.0104 | 0.0019      | 0.0102 |
|                   | 30        | 0.0068 | 0.0018      | 0.0100 | 0.0021      | 0.0094 |
|                   | 40        | 0.0064 | 0.0018      | 0.0092 | 0.0021      | 0.0086 |
|                   | 50        | 0.0060 | 0.0018      | 0.0084 | 0.0023      | 0.0074 |
|                   | 70        | 0.0047 | 0.0018      | 0.0058 | 0.0018      | 0.0058 |
| Total             |           |        |             | 0.0932 |             | 0.0888 |
| $\Sigma$ EDA      |           |        |             | 0.268  |             | 0.283  |
| $\Sigma$ ESA (Ba) |           |        |             | 0.744  |             |        |
| $\Sigma$ ESA (Co) |           |        |             |        |             | 0.804  |

Note. The table also gives the total equivalent sorbed amounts ( $\Sigma$  ESA) of the sorbed ions and the total equivalent depleted amounts ( $\Sigma$  EDA) of depleted cations for sorption on kaolinite. All calculations are based on ToF-SIMS measurements

70 Å depth. Unlike the sorbed amounts of  $Ba^{2+}$  ions, those of  $Co^{2+}$  show a continuous decrease below the outermost clay surface up to the analyzed depth of 70 Å. Based on the total equivalent sorbed amounts (ESA, Table 2), it is seen that  $Co^{2+}$  is sorbed in a slightly larger amount. However, taking the uncertainty associated with the measured values into consideration would also indicate no significant difference in the total sorbed amounts of  $Co^{2+}$  and  $Ba^{2+}$  ions on kaolinite.

Furthermore, Table 2 indicates that the total ESA of each of  $Ba^{2+}$  and  $Co^{2+}$  exceed the corresponding total EDA of the depleted ions. This probably indicates that, in addition to ion exchange, other sorption mechanisms might be operating, for example, incorporation of the sorbed ions in structural defects possessing permanent negative charge and hydrolytic sorption, which can be described by the following equation [7]:



The reaction could be figured out as an ion-exchange reaction that takes place when the sorbed ion is in its unhy-

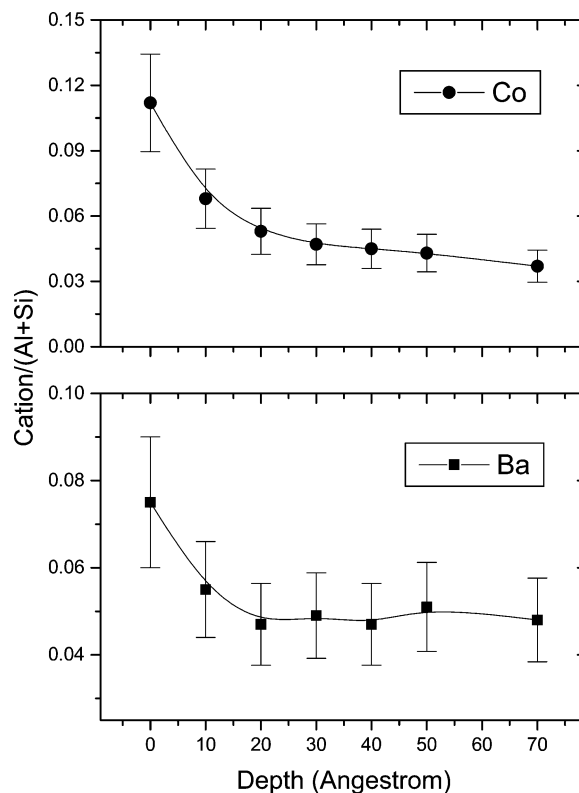


Fig. 4. Variation of the sorbed amounts (cation/(Al+Si)) of  $Ba^{2+}$  and  $Co^{2+}$  with depth (Å) in kaolinite lattice. The fits are used to guide the eye.

dolyzed form. Ion exchange on sites having permanent negative charges and complexation of  $Co^{2+}$  to hydroxyl-edge groups of kaolinite were reported in earlier studies [8,9]. Another sorption mechanism that can be of importance is binding to coordinatively unsaturated  $O^{2-}$  groups that are exposed at the clay surface and that can complete their coordination sphere by holding the sorbed ion ( $M^{n+}$ ) as  $-O_xM$  groups. Based on EXAFS results, the formation of oxide- or hydroxide-bridged multinuclear surface complexes on kaolinite from undersaturated solutions of  $Co^{2+}$  was reported [10,11]. According to the same study, increasing the concentration of  $Co^{2+}$  leads to the formation of  $Co(OH)_2$  precipitate. The formation of hydrotalcite-like precipitates when  $Co^{2+}$  ions were allowed to contact kaolinite for prolonged time periods was also documented [12]. According to our earlier studies, based on Gibbs energy of sorption, the uptake of  $Co^{2+}$  and  $Ba^{2+}$  on kaolinite was suggested to be of an electrostatic nature (mainly ion-exchange type) [13,14]. In addition to electrostatic sorption, chemisorption of  $Ba^{2+}$  on kaolinite was also reported upon pretreatment of the clay with sea water [15].

XRPD was used to study the possible structural changes of kaolinite upon sorption. The XRD diagrams of natural and Ba- and Co-sorbed kaolinite are shown in Fig. 1. The peak intensities in each spectrum were normalized to the corresponding intensity of the quartz (101) peak, which showed no intensity changes upon sorption, as given in Table 3. As the table shows, sorption of  $Ba^{2+}$  and  $Co^{2+}$  has caused slight

reductions in the intensities of the kaolinite (001) and (002) features. This implies that the basal spacing of the clay was not significantly affected by sorption, consistent with the fact that the contribution of interlayer sites of kaolinite to sorption is limited. The SEM images of the clay taken at different magnifications ( $\times 50,000$ ,  $\times 100,000$ ,  $\times 150,000$ ) suggested that the morphology of kaolinite seems to be retained upon sorption of both cations. The EDS analysis of Ba (*L* line) and Co (*K* line) showed that the average atomic percentage ( $\pm$ S.D.) of Ba and Co on kaolinite surface was  $0.49 \pm 0.11$  and  $0.61 \pm 0.19$ , respectively. This fact points to a limited retention of both ions by the natural kaolinite clay.

Table 3

The intensities (normalized to the quartz (101) peak) of major peaks corresponding to the main mineralogical fractions in natural and Ba- and Co-sorbed kaolinite, determined using XRPD measurements

| Mineral fraction | Na kaolinite |           | Ba-kaolinite |           | Co-kaolinite |           |
|------------------|--------------|-----------|--------------|-----------|--------------|-----------|
|                  | $d_{hkl}$    | Intensity | $d_{hkl}$    | Intensity | $d_{hkl}$    | Intensity |
| Quartz (101)     | 3.34         | 100       | 3.35         | 100       | 3.35         | 100       |
| Kaolinite (001)  | 7.15         | 112       | 7.20         | 105       | 7.20         | 81        |
| Kaolinite (002)  | 3.57         | 128       | 3.59         | 124       | 3.59         | 98        |
| Kaolinite (110)  | 4.35         | 25        | 4.38         | 24        | 4.38         | 23        |
| Quartz (100)     | 4.25         | 29        | 4.27         | 31        | 4.27         | 30        |
| Kaolinite (020)  | 4.45         | 19        | 4.47         | 19        | 4.47         | 19        |

The mapping SEM analysis, given in Fig. 5a, 5b for the Co- and Ba-sorbed clay samples, indicated that  $\text{Co}^{2+}$  ions were distributed more homogeneously on the surface than  $\text{Ba}^{2+}$  ions, which seemed to be occasionally localized on certain sites more than the others. Both  $\text{Ba}^{2+}$  and  $\text{Co}^{2+}$  ions failed to show a distinguishable preference toward binding to regions rich in aluminol or silanol groups.

#### 4. Conclusion

In this study the surface-sensitive technique ToF-SIMS was used for depth profiling of the sorption of  $\text{Ba}^{2+}$  and  $\text{Co}^{2+}$  on natural Turkish clay rich in kaolinite. The detailed analysis of various ions at different points on the clay surface have shown that in addition to ion exchange, other sorption mechanisms might be operative. XRPD results supports the fact that sorption on interlayer positions of kaolinite have a limited contribution to sorbed amount of both cations. SEM micrographs indicated that the morphology of the clay retained its identity upon sorption of both ions. EDS data have shown that kaolinite possess a limited sorption capacity towards both cations.

#### Acknowledgments

The authors thank the British Council at Ankara for the financial help through the link program, and the Center of Material Research at Izmir Institute of Technology for help in the SEM measurements.

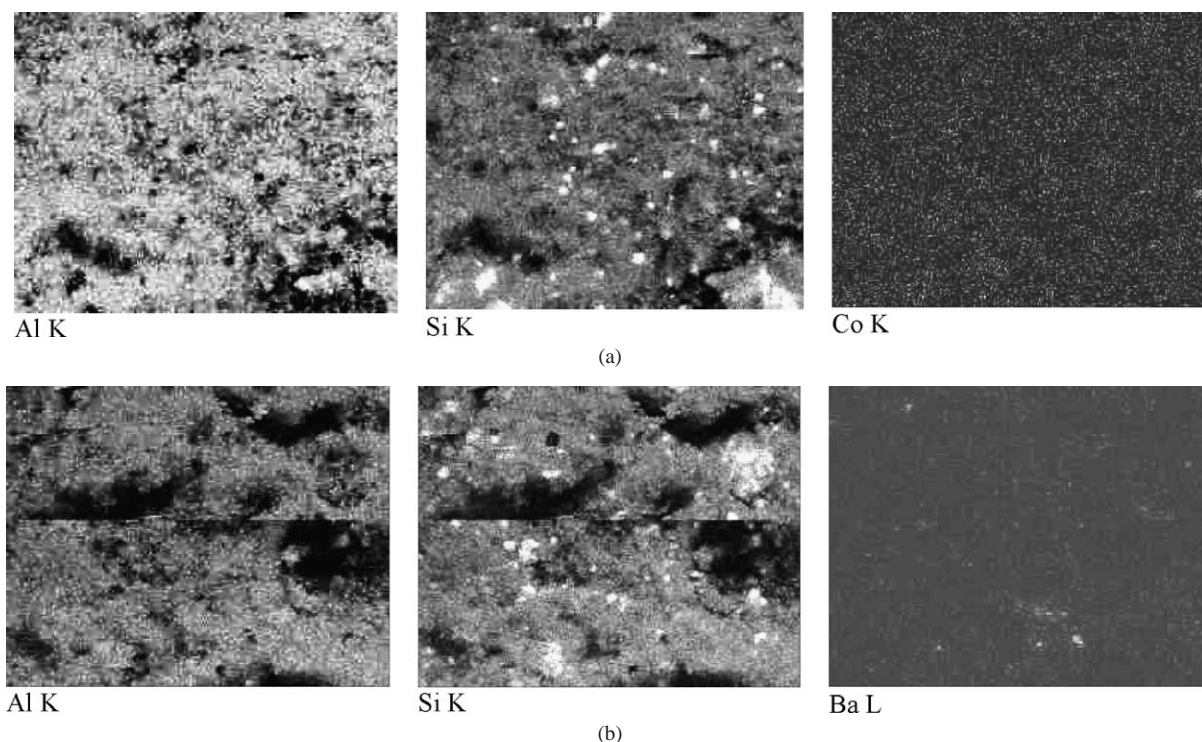


Fig. 5. SEM mapping images of Al, Si, and Co or Ba in (a) Co-sorbed kaolinite and (b) Ba-sorbed kaolinite.

## References

- [1] J.I. Drever, *The Geochemistry of Natural Waters*, Prentice–Hall, Englewood Cliffs, NJ, 1982.
- [2] T. Shahwan, S. Sayan, H.N. Erten, L. Black, K.R. Hallam, G.C. Allen, *Radiochim. Acta* 88 (2000) 681.
- [3] T. Shahwan, H.N. Erten, *Radiochim. Acta* 89 (2001) 799.
- [4] T. Shahwan, H.N. Erten, L. Black, G.C. Allen, *Sci. Total Environ.* 226 (1999) 255.
- [5] D. Briggs, M.P. Seah, *Practical Surface Analysis*, vol. 2. Ion and Neutral Spectroscopy, Wiley, New York, 1996.
- [6] G.R. Sparrow, in: *Proc. 25th Conference of Mass Spectrometry and Allied Topics*, May 29–June 3, 1977, Washington, DC.
- [7] K.H. Lieser, *Radiochim. Acta* 70/71 (1995) 355.
- [8] J. Ikhsan, B.B. Johnson, J.D. Wells, *J. Colloid Interface Sci.* 217 (1999) 403.
- [9] M.J. Angove, B.B. Johnson, J.D. Wells, *J. Colloid Interface Sci.* 204 (1998) 93.
- [10] P.A. O'Day, G.E. Brown Jr., G.A. Parks, *J. Colloid Interface Sci.* 165 (1994) 269.
- [11] H.A. Thompson, G.A. Parks, G.E. Brown Jr., *Geochim. Cosmochim. Acta* 63 (1999) 1767.
- [12] H.A. Thompson, G.A. Parks, G.E. Brown Jr., *J. Colloid Interface Sci.* 222 (2000) 241.
- [13] T. Shahwan, H.N. Erten, *J. Radioanal. Nucl. Chem.* 260 (1) (2004) 43.
- [14] T. Shahwan, H.N. Erten, *J. Radioanal. Nucl. Chem.* 241 (1) (1999) 151.
- [15] R. Kleven, J. Alstad, *J. Pet. Sci. Eng.* 15 (1996) 181.